

Xanthate-Mediated Controlled Radical Polymerization of *N*-Vinylindole Derivatives

Yuya Maki,[†] Hideharu Mori,^{*,†} and Takeshi Endo^{*,‡}

Department of Polymer Science and Engineering, Faculty of Engineering, Yamagata University, 4-3-16, Jonan, Yonezawa 992-8510, Japan, and Molecular Engineering Institute, Kinki University, Iizuka, Fukuoka 820-8555, Japan

Received December 12, 2006; Revised Manuscript Received June 12, 2007

ABSTRACT: The polymerization of three *N*-vinylindole derivatives, *N*-vinylindole (NVIn), 2-methyl-*N*-vinylindole (2MNVIn), and 3-methyl-*N*-vinylindole (3MNVIn), were carried out by reversible addition–fragmentation chain transfer (RAFT)/macromolecular design via interchange of xanthate (MADIX) process. Five chain transfer agents (CTAs), *S*-benzyl-*O*-ethylthiocarbonate (CTA 1), *O*-ethyl-*S*-(1-phenylethyl)dithiocarbonate (CTA 2), *O*-ethyl-*S*-[(2-cyano)prop-2-yl]dithiocarbonate (CTA 3), benzyl 1-pyrrolicarboxodithioate (CTA 4), and benzyl dithiobenzoate (CTA 5), were compared for these polymerizations with 2,2'-azobis(isobutyronitrile) as an initiator. The xanthate-type RAFT agent (CTA 2) is the most efficient for obtaining poly(2MNVIn) with controlled molecular weights ($M_n = 1700$ – $19\,400$) and narrow molecular weight distributions ($M_w/M_n = 1.20$ – 1.40). The effects of several parameters, such as solvent, temperature, monomer concentration, and CTA-to-initiator molar ratio, were examined in order to determine the conditions leading to optimal control of the polymerization. The resulting polymers gave clear spectroscopic evidence of the formation of charge-transfer complexes with efficient sensitizers, such as 7,7,8,8-tetracyanoquinodimethane (TCNQ), tetracyanoethylene (TCNE), and 2,3-dichloro-5,6-dicyano-1,4-benzoquinone (DDQ), for photoconductivity. The poly(2MNVIn)s obtained by RAFT polymerization showed molecular weight dependence on the glass transition temperature ($T_g = 150$ – 190 °C) and thermal stability ($T_d^{10} = 300$ – 430 °C).

Introduction

Indoles are aromatic heterocyclic compounds, which are a common component or precursor of alkaloids and other neutral products.^{1–4} The indole ring system represents one of the most important structural components in many pharmaceutical agents, which is mainly due to the great structural diversity of biologically active indoles.^{5–7} Indeed, numerous compounds containing this ring have been developed, and some substitutes have been referred as a privileged structure because of their ability to bind many receptors with high affinity. The indole ring system is also an attractive scaffold for combinatorial synthesis.^{5,8}

In addition to their wide variety of biological applications, the photochemistry of indole derivatives has been studied extensively.⁹ The indole ring system is used as a photochemical precursor, and a variety of photoinduced reactions have been reported, which involve photorearrangement, photocycloaddition, and photocyclization.^{9–12} Indole derivatives have also been used as ligands to form a number of transition metal complexes.^{13–15} The incorporation of an indole unit into a luminescent transition metal complex, such as rhenium(I) and ruthenium(II) polypyridine indole conjugates, has been developed to create probes for indole-binding biomaterials.^{16,17}

During recent years, considerable attention has been paid to polymers containing indole derivatives in the main and side chains. Polyindole and poly(*N*-alkylindole) are electroactive polymers and are regarded as heteroatom-containing conducting polymers, which can be obtained by electrochemical oxidation

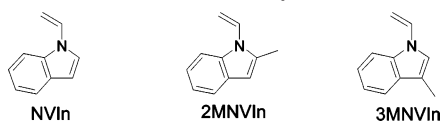
of indole or chemical oxidation using FeCl_3 or CuCl_2 .^{18–20} A variety of polymers having indole groups in the side chains have been reported, including poly(*N*-vinylindole)s,^{21–24} polyacrylates,^{25,26} polymethacrylates,^{26–29} and polyacetylene³⁰ derivatives. Among them, increasing attention has been paid to poly(*N*-vinylindole) derivatives as novel photorefractive polymers because of good photoconductivity due to the low ionization potential of the pendant indole unit and relatively low glass transition temperature (T_g).²² Precise control in chemical structure, polymer architecture, conformation, location, and stacking of the indole units is essential because it affects their properties and morphology. *N*-Vinylindole (NVIn) can be polymerized in the presence of organic electron acceptors, such as 2,3-dichloro-5,6-dicyano-*p*-benzoquinone and *p*-chloranil,²³ and free radical polymerization using an azo-type initiator was also used for the production of poly(NVIn) derivatives.^{22,31} Cationic initiators, such as $\text{BF}_3 \cdot \text{OEt}_2$, HI, and HI/I_2 , readily polymerize NVIn derivatives.²² The copolymerization of NVIn with electron acceptors can give copolymers with peculiar structures and properties, in which the formation of a charge-transfer complex plays an important role in manipulating the copolymerization behavior.^{30,32}

We now report the synthesis of poly(NVIn) derivatives with predetermined molecular weights and narrow polydispersity by xanthate-mediated controlled radical polymerization. In order to understand the polymerization mechanism of this class of monomers, we selected three different *N*-vinylindole derivatives, *N*-vinylindole (NVIn), 2-methyl-*N*-vinylindole (2MNVIn), and 3-methyl-*N*-vinylindole (3MNVIn), as shown in Scheme 1. Controlled/living radical polymerization has allowed synthesizing various functional polymers with predetermined molecular weights, narrow molecular weight distribution, and controlled architectures, such as graft and block copolymers, by a facile approach.^{33–36} However, the controlled radical polymerization

* To whom correspondence should be addressed: e-mail h.mori@yz.yamagata-u.ac.jp and tendo@me-henkel.fuk.kindai.ac.jp, phone +81-238-26-3765, Fax +81-238-26-3092.

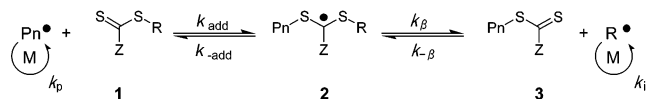
[†] Yamagata University.

[‡] Kinki University.

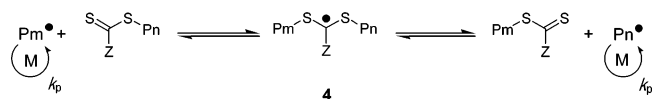
Scheme 1. Structures of *N*-Vinylindole Derivatives

Scheme 2. Basic Reaction Steps of Reversible Addition–Fragmentation Chain Transfer (RAFT) Process

Pre-equilibrium (Reversible chain transfer)



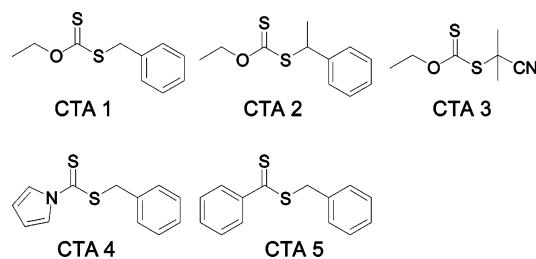
Main equilibrium (Chain equilibration)



of *N*-vinyl and *O*-vinyl monomers had been difficult because the generated radical species are highly reactive due to their nonconjugated nature and strong electron-donating pendant groups. Among various controlled radical polymerizations, in this study, we selected reversible addition–fragmentation chain transfer (RAFT) polymerization,^{36–40} because of its versatility with respect to monomer type and reaction conditions. The RAFT process is generally accomplished by performing a radical polymerization in the presence of a thiocarbonylthio compound, such as dithioesters, dithiocarbamates, trithiocarbonates, and xanthates, which all act as reversible chain transfer agents (CTAs). When xanthates are employed, the terminology MADIX (macromolecular design via the interchange of xanthates) is frequently used to describe the process.^{39,40} Recently, we published the first report of the xanthate-mediated controlled radical polymerization of *N*-vinylcarbazole,⁴¹ which is a typical *N*-vinyl monomer. Dithiocarbonates (xanthates) are also useful for controlling the radical polymerization of *O*-vinyl and *N*-vinyl monomers, such as vinyl acetate^{42–44} and *N*-vinylpyrrolidone.^{44,45} Both MADIX and RAFT processes are based upon the generally accepted reversible addition–fragmentation chain transfer mechanism between an active and a dormant species. To achieve control of the radical polymerization via the RAFT/MADIX process, a delicate balance of the forward and reverse rates of addition (k_{add} and $k_{-\text{add}}$) and fragmentation (k_{β} and $k_{-\beta}$), together with the rates of reinitiation (k_i) and propagation (k_p), is required, as shown in Scheme 2.

Although the stabilizing effect of NVIn ($Q = 0.53$, $e = -1.30$) is slightly higher than that of *N*-vinylcarbazole ($Q = 0.26$, $e = -1.29$) with a similar electron-donating property, NVIn has been reported to have a lower activation energy ($E_A = 17.5 \text{ kJ/mol}^{-1}$) than that of *N*-vinylcarbazole (27.4 kJ/mol), suggesting that the propagating NVIn radical possesses higher reactivity.²¹ Because the NVIn propagating radical is a reactive species having a higher electron density at the radical center, the fragmentation of the adduct radical (intermediate RAFT radical) is thought to be slow. In this study, we mainly employed the xanthate-type CTA because it increases the electron density at the radical center, which may lead to destabilization of the intermediate radicals **2** and **4** and an increase in the fragmentation rate. The electron-donating *O*-alkyl substituents may lead to stabilization of the polymeric thiocarbonylthio product **3** through their conjugation with the $\text{C}=\text{S}$ double bond, which lowers the rate of addition of the propagating radicals to the sulfur atom and, consequently, the overall rate of chain transfer.^{37,43,44,46} With this in mind, we attempted to find a

Scheme 3



suitable CTA and conditions to provide the controlled radical polymerization of NVIn derivatives.

Experimental Section

Materials. Indole (Kanto Chemical, 98%), 2-methylindole (Merck, 98%), and 3-methylindole (Tokyo Kasei Kogyo, 98%) were used as received. 2,2'-Azobis(isobutyronitrile) (AIBN, Kanto Chemical, 97%) was purified by recrystallization from ethanol. 1,2-Dichloromethane (Kanto Chemical, 99%), *N,N*-dimethylformamide (dehydrated DMF, Kanto Chemical, 99.5%), 1,4-dioxane (dehydrated, Kanto Chemical, 99.5%), KOH (Kanto Chemical, 99%), tetrabutylammonium bromide (Kanto Chemical, 98%), 7,7,8,8-tetracyanoquinodimethane (TCNQ, Tokyo Kasei Kogyo, 99%), tetracyanoethylene (TCNE, Tokyo Kasei Kogyo, 98%), 2,3-dichloro-5,6-dicyano-1,4-benzoquinone (DDQ, Tokyo Kasei Kogyo, 97%), and hydroquinone (Kanto Chemical, 98%) were used as received. Toluene (Kanto Chemical, 99%) was distilled over sodium wire. Other materials were used without further purification.

Synthesis of Chain Transfer Agents (CTAs). Five different CTAs were prepared in this study, as shown in Scheme 3. *S*-Benzyl-*O*-ethyl dithiocarbonate (CTA 1) was synthesized by the reaction of potassium ethyl xanthogenate and benzyl bromide according to a procedure reported in the literature.^{41,47} The synthesis of *O*-ethyl-*S*-(1-phenylethyl) dithiocarbonate (CTA 2) was conducted similar to the preparation of CTA 1, replacing benzyl bromide with (1-phenylethyl)benzene.^{41,48,49} The CTA 1 and CTA 2 were finally purified by column chromatography on silica with *n*-hexane as the eluent to afford the corresponding products as yellow oil.⁴¹ The synthesis of *O*-ethyl-*S*-[(2-cyano)prop-2-yl] dithiocarbonate (CTA 3) was carried out by the reaction of AIBN and *O,O*-diethyl bisxanthate derived from potassium ethyl xanthogenate.^{50,51} Benzyl 1-pyrrolicarboxy dithioate (CTA 4)^{52,53} and benzyl dithiobenzoate (CTA 5)^{54,55} were prepared according to the procedures reported previously. The CTA 3 and CTA 4 were finally purified by column chromatography on silica with *n*-hexane/ethyl acetate (10/1) as the eluent. The CTA 5 was purified by vacuum distillation using a glass tube oven (Shibata GTO-250RS) to give a red oil. The elemental analyses of the CTAs gave calculated purities of >99% for CTA 1, CTA 2, CTA 3, and CTA 4 and 98% for CTA 5.

Synthesis of *N*-Vinylindole Derivatives. 2-Methyl-*N*-vinylindole (2MNvIn) was obtained by the *N*-alkylation of 2-methylindole, followed by the elimination reaction.^{56,57} Under the nitrogen atmosphere, 2-methylindole (5.0 g, 38 mmol) was added to an intensely stirred mixture of 1,2-dichloroethane (100 g, 1.0 mol), tetrabutylammonium bromide (0.25 g, 0.8 mmol), KOH (14 g, 250 mmol), and K_2CO_3 (11 g, 80 mmol) at room temperature. The stirring was continued at 40–50 °C for 72 h. After cooling, the inorganic material was filtered off, and the organic solvent was removed by evaporation. A mixture of the condensate, which corresponds to crude 3-chloroethyl 2-methylindole (5.0 g, 26 mmol), KOH (2.2 g, 240 mmol), and hydroquinone (30 mg, 0.27 mmol), was placed in toluene (100 mL) and refluxed for 3 h. After the toluene solution was evaporated under reduced pressure, the organic material was extracted from the reaction mixture by means of methylene chloride ($3 \times 30 \text{ mL}$) with water (50 mL). The extract was then dried over anhydrous MgSO_4 and filtered, and the solvent was evaporated to give a dark red liquid. The crude product was distilled under vacuum (90 °C/0.5 mmHg), followed by the purification by silica gel chromatography eluted with *n*-hexane/

ethyl acetate = 5/1 (volume ratio) to give 2MNVIn as a pale yellow liquid (2.8 g, yield 68%, lit.⁵⁷ 68%). *N*-Vinylindole (NVIn) and 3-methyl-*N*-vinylindole (3MNVIn) were synthesized from indole and 3-methylindole, in a manner similar to 2MNVIn, respectively. The yield was 73% for NVIn and 60% for 3MNVIn. The ¹H and ¹³C NMR spectra of the monomers are shown in Figures S1, S3, and S5 (see Supporting Information).

General Polymerization Procedure. All polymerizations were carried out with AIBN as an initiator in a degassed sealed tube. A representative example is as follows: 2MNVIn (0.31 g, 2.0 mmol), CTA 2 (4.5 mg, 0.020 mmol), AIBN (1.6 mg, 0.010 mmol), and dry 1,4-dioxane (1.0 mL) were placed in a dry glass ampule equipped with a magnetic stirring bar, and the solution was then degassed by three freeze–evacuate–thaw cycles. After the ampule was flame-sealed off under vacuum, it was stirred at 60 °C for 48 h. The characteristic pale yellow color remained during the polymerization. The reaction was stopped by rapid cooling with liquid nitrogen. For the determination of the monomer conversion, the ¹H NMR spectrum of the polymerization mixture collected just after the polymerization was measured in CDCl₃ at room temperature, and the integration of the monomer CH₂=CH resonance at around 5.1 and 5.4 ppm was compared with the sum of the peak intensity of the indole heterocyclic moiety (1H) in the polymer and the monomer at around 5.4–6.5 ppm. Conversion determined by this method was 50%. The polymer obtained was purified by reprecipitation from a chloroform solution into a large excess of methanol, and the resulting product was dried at room temperature under vacuum: yield 0.16 g, 52%. The resulting product was soluble in dichloromethane, toluene, tetrahydrofuran, chloroform, and DMF while insoluble in acetone, hexane, MeOH, and water. ¹H NMR (CDCl₃): δ 0.1–1.5 (2H, CH₂ in the polymer main chain), 1.5–2.5 (3H, CH₃ in the indole residue), 2.5–4.5 (1H, CH in the polymer main chain), 5.4–6.5 (1H, CH in the indole residue), and 6.5–8.0 ppm (4H, aromatic protons). ¹³C NMR (CDCl₃): δ 10–16, 35–45, 47–53, 100–105, 107–112, 117–125, 126–130, and 132–139 ppm. The ¹H NMR and ¹³C NMR spectra of the polymer are shown in Figure S4 (see Supporting Information).

The theoretical number-average molecular weight on conversion is defined as follows:

$$M_n(\text{theor}) = \frac{[\text{monomer}]_0}{[\text{CTA}]_0 + 2f[\text{I}]_0(1 - e^{-k_d t})} \times M_{\text{monomer}} \times \text{conv} + M_{\text{CTA}} \quad (1)$$

in which M_{CTA} and M_{monomer} are molecular weights of CTA and the monomer (NVIn, 2MNVIn, 3MNVIn), and $[\text{monomer}]_0$ and $[\text{CTA}]_0$ are the initial concentrations of monomer and CTA, respectively. The right side of the denominator accounts for radicals derived from the initiator with an initial concentration $[\text{I}]_0$ at time t with a decomposition rate, k_d . The initiator efficiency is represented by f . In an ideal RAFT process, the polymer directly derived from the initiators is minimal, and thus the second term in the denominator becomes negligible and eq 1 can be simplified to eq 2.

$$M_n(\text{theor}) = \frac{[\text{monomer}]_0}{[\text{CTA}]_0} \times M_{\text{monomer}} \times \text{conv} + M_{\text{CTA}} \quad (2)$$

For the kinetic study, a mixed solution of 2MNVIn (1.86 g, 12 mmol), CTA 2 (27 mg, 0.12 mmol), AIBN (9.6 mg, 0.060 mmol), and dry 1,4-dioxane (6.0 mL) was typically divided into six glass ampules, and each solution was then degassed by three freeze–evacuate–thaw cycles. The ampules were sealed by a flame under vacuum and then placed in a thermostatic oil bath at 60 °C for the desired time. The monomer conversion was determined by the ¹H NMR spectrum of the polymerization mixture.

Chain Extension Using Poly(2-methyl-*N*-vinylindole) as Macro-CTA. For the chain extension experiments, poly(2MNVIn) having lower molecular weights was prepared according to the following procedure. 2MNVIn (0.31 g, 2.0 mmol), CTA 2 (4.5 mg, 0.020 mmol), AIBN (1.6 mg, 0.010 mmol), and dry 1,4-dioxane (1.0 mL)

were placed in an ampule. After three freeze–evacuate–thaw cycles, the polymerization mixture was stirred at 60 °C for 12 h, and the monomer conversion was 13%. The product was purified by precipitation in methanol and then isolated by filtration. Finally, the resulting poly(2MNVIn) was dried under vacuum at room temperature (yield = 16%). The M_n of the resulting poly(2MNVIn), as determined by size-exclusion chromatography (SEC), was 2300, and the polydispersity index was 1.25.

A representative example of the chain extension experiment is as follows: the xanthate-terminated poly(2MNVIn) (macro-CTA) (46 mg, 0.020 mmol; $M_n = 2300$, $M_w/M_n = 1.25$), 2MNVIn (0.31 g, 2.0 mmol), AIBN (1.6 mg, 0.010 mmol), and dry 1,4-dioxane (1.0 mL) were placed in a dry ampule, and the solution was then degassed by three freeze–evacuate–thaw cycles. The polymerization was conducted at 60 °C for 24 h. Conversion was 26%, and the polymer yield determined from the methanol insoluble sample was 29%. The resulting poly(2MNVIn) had an M_n (as determined by SEC) of 8900 and a polydispersity index of 1.35.

Instrumentation. ¹H (400 MHz) and ¹³C NMR (100 MHz) spectra were recorded with a JEOL EX-400. The number-average molecular weight (M_n) and molecular weight distribution (M_w/M_n) were estimated by size-exclusion chromatography (SEC) using a system consisting of a Tosoh DP-8020 pump and a Viscotek TDA model-301 triple detector array (RI, viscosity, and RALLS; wavelength = 670 nm) at 40 °C. The column set was as follows: four consecutive columns [Tosoh TSK-GELs (bead size, exclusion limited molecular weight): GMH_{XL} (9 μm, 4 × 10⁸), G4000H_{XL} (5 μm, 4 × 10⁵), G3000H_{XL} (5 μm, 6 × 10⁴), G2500H_{XL} (5 μm, 2 × 10⁴), 30 cm each] and a guard column [TSK-guard column H_{XL}-H, 4.0 cm] eluted with THF at a flow rate of 1.0 mL/min. The excess refractive index increment $[dn/dc = 0.263$ for poly(2MNVIn)] was measured in THF at 25 °C using a DRM 1021 differential refractometer operating at 633 nm.

The UV–vis spectra were recorded with a JASCO V-550-DS spectrophotometer. Thermogravimetric analysis (TGA) was performed on a SEIKO TGA/6200 at a heating rate of 10 °C/min under N₂. For differential scanning calorimetry (DSC) measurements, a SEIKO DSC/6200 apparatus was used (heating rate: 10 °C/min; cooling rate: 20 °C/min). Samples were heated from 30 to 200 °C at a rate of 10 °C/min, kept for 5 min, and cooled at a rate of 20 °C/min. The data collection was carried out in the second heating process, and the glass transition temperature (T_g) was taken to be the midpoint—the temperature corresponding to half of the endothermic shift. The calorimeter was calibrated with an indium standard. Elemental analysis was carried out on a Perkin-Elmer 2400II CHNS/O analyzer.

Results and Discussion

Conventional Radical Polymerization of *N*-Vinylindole Derivatives. Several attempts to synthesize poly(*N*-vinylindole), poly(NVIn), derivatives by radical polymerizations have appeared in the literature, although inconsistent tendencies were reported by several groups. Priola et al.²⁴ reported that radical polymerization of NVIn produced low molecular weight products with relatively low yield, unless high monomer and initiator concentrations were used. This is due to a backbiting attack of the propagating species at the 2-position of the indole ring, resulting in the formation of cyclic indole units. Brustolin et al. demonstrated the preparation of poly(NVIn) having relatively high molecular weights at low initiator concentration, while the polymer yield was low even for longer polymerization time.²² They also claimed that conventional radical polymerization of 2-methyl-*N*-vinylindole, 2MNVIn, gave predominantly low molecular weight products, even though the presence of a methyl group at the 2-position of the indole ring should prevent chain termination by the cyclization reactions. In contrast, Priola et al.²⁴ demonstrated that the presence of a methyl group at the 2-position increased both the conversion and molecular weight

Table 1. Conventional Radical Polymerization of *N*-Vinylindole (NVIn), 2-Methyl-*N*-vinylindole (2MNVIn), and 3-Methyl-*N*-vinylindole (3MNVIn) Using 2,2'-Azobis(isobutyronitrile) (AIBN) in 1,4-Dioxane at 60 °C^a

run	monomer	time (h)	conv ^b (%)	yield ^c (%)	M_n^d	M_w/M_n^d
1	NVIn	24	33	34	10 400	2.23
2	NVIn	48	77	69	12 000	3.54
3	2MNVIn	24	69	60	30 200	2.05
4	2MNVIn	48	93	81	33 000	3.87
5	3MNVIn	24	1 <			
6	3MNVIn	48	15			

^a $[M]_0/[AIBN]_0 = 200/1$, $[AIBN]_0 = 7.8 \times 10^{-3}$ mol/L, $[monomer]_0 = 1.6$ mol/L. ^b Calculated by ¹H NMR in CDCl₃. ^c MeOH-insoluble part. ^d Number-average molecular weight (M_n) and molecular weight distribution (M_w/M_n) were measured by size-exclusion chromatography (SEC) using polystyrene standards in THF.

under conventional radical polymerization. From the ¹³C NMR analysis of the resulting polymers, they suggested the formation of unfavorable cyclic structures during the polymerizations of NVIn and 3-methyl-*N*-vinylindole (3MNVIn), whereas a regular vinyl polymerization of 2MNVIn took place without any evidence of the cyclization. In order to clarify these points, we first compared the conventional radical polymerization of three different *N*-vinylindole derivatives, NVIn, 2MNVIn, and 3MNVIn (Scheme 1), in the presence of AIBN as an initiator. These *N*-vinylindole derivatives were synthesized by the combination of *N*-alkylation and elimination reactions according to the previously reported procedure.^{56,57}

The polymerization of NVIn was conducted with AIBN at 60 °C at $[M]_0/[AIBN]_0 = 200$ in order to find conditions for obtaining polymeric product having relatively high molecular weight with sufficient yield. As shown in Table 1, the polymerization produced poly(NVIn) having a moderate molecular weight ($M_n = 10\,400$, $M_w/M_n = 2.23$), while only 33% conversion was achieved even after 24 h. Longer polymerization time (48 h) led to higher conversion with slight increases in the molecular weight and polydispersity. When 2MNVIn was polymerized at 60 °C for 24 h, a polymer having relatively high molecular weights ($M_n = 30\,200$) was obtained with high conversion (69%, as determined by ¹H NMR spectroscopy). Almost full conversion (93%) was obtained for the polymerization for 48 h. Higher molecular weight of poly(2MNVIn) than that of poly(NVIn) could account for an inherent tendency of the propagating poly(NVIn) radical to undergo chain transfer reactions. They probably involve a backbiting attack of the propagating radical at the 2-position of the indole ring, while the presence of a methyl group at the 2-position prevents the chain transfer reactions.²⁴ In agreement with previous results from Brustolin et al.,²² radical polymerization of 3MNVIn with AIBN gave only poor yield. This may be due to the high π electron density of the vinyl group in 3MNVIn (see Supporting Information, Table S1), suggesting that 3MNVIn is much more susceptible to cationic polymerization than radical polymerization. On the basis of these preliminary results, we selected 2MNVIn for our further investigations toward the precise synthesis of poly(*N*-vinylindole) derivatives having low polydispersity and controlled molecular weights. In this context, we initially present RAFT polymerization of a monosubstituted *N*-vinylindole, 2MNVIn. We then show preliminary results of radical polymerization of NVIn using different CTAs for comparison.

RAFT Polymerization of 2-Methyl-*N*-vinylindole (2MNVIn) Using Different CTAs. It has been demonstrated that successful implementation of the RAFT process requires careful

Table 2. Polymerization of 2-Methyl-*N*-vinylindole (2MNVIn) Using Different Chain Transfer Agents (CTAs) in 1,4-Dioxane at 60 °C^a

run	CTA ^b	time (h)	conv ^c (%)	M_n		M_w/M_n^e
				theory ^d	SEC ^e	
1	CTA 1	24	40	7200	6200	1.31
2	CTA 2	24	26	4300	3400	1.25
3	CTA 3	24	28	3600	3400	1.36
4	CTA 4	24	44	7300	7400	1.76
5	CTA 5	24	21	3500	3200	1.40
6	CTA 1	48	72	11500	8500	1.56
7	CTA 2	48	50	8100	6300	1.31
8	CTA 3	48	56	9000	10800	1.39
9	CTA 4	48	65	10500	9000	1.59
10	CTA 5	48	55	8900	4900	1.56

^a $[2MNVIn]_0/[CTA]_0/[AIBN]_0 = 200/2/1$, $[AIBN]_0 = 7.8 \times 10^{-3}$ mol/L, $[CTA]_0 = 1.6 \times 10^{-2}$ mol/L, $[2MNVIn]_0 = 1.6$ mol/L, where AIBN = 2,2'-azobis(isobutyronitrile), 2MNVIn = 2-methyl-*N*-vinylindole. ^b CTA 1 = *S*-benzyl-*O*-ethylthiocarbonate, CTA 2 = *O*-ethyl-*S*-(1-phenylethyl)dithiocarbonate, CTA 3 = *O*-ethyl-*S*-[(2-cyano)prop-2-yl]dithiocarbonate, CTA 4 = benzyl 1-pyrrolocarbodithioate, CTA 5 = benzyl dithiobenzoate (Scheme 3). ^c Calculated by ¹H NMR in CDCl₃. ^d The theoretical molecular weight ($M_{n,theory}$) = (MW of 2MNVIn) \times $[2MNVIn]_0/[CTA]_0 \times conv +$ (MW of CTA). ^e Number-average molecular weight (M_n) and molecular weight distribution (M_w/M_n) were measured by size-exclusion chromatography (SEC) using polystyrene standards in THF.

selection of the CTA and reaction conditions, depending upon the monomer. In this study, three xanthate-type mediating agents having different leaving groups, *S*-benzyl-*O*-ethylthiocarbonate (CTA 1), *O*-ethyl-*S*-(1-phenylethyl)dithiocarbonate (CTA 2), and *O*-ethyl-*S*-[(2-cyano)prop-2-yl]dithiocarbonate (CTA 3), were selected as the CTA (Scheme 3). The effect of the R substitute on the effectiveness of xanthate derivatives ($S=C(OEt)S-R$) was initially investigated on the polymerization of 2MNVIn. We also employed dithiocarbamate-type (CTA 4) and dithioester-type (CTA 5) mediating agents for comparison. CTA 1, CTA 4, and CTA 5 have the same R group, which yields a benzyl radical species upon fragmentation.

The polymerization of 2MNVIn was conducted with different CTAs and AIBN as an initiator at $[M]_0/[CTA]_0 = 100$ using the ratio of AIBN to CTA of 1:2 ($[M]_0/[CTA]_0/[AIBN]_0 = 200/2/1$). These conditions correspond to $[AIBN]_0 = 7.8 \times 10^{-3}$ mol/L, $[CTA]_0 = 1.6 \times 10^{-2}$ mol/L, and $[2MNVIn]_0 = 1.6$ mol/L. The results are summarized in Table 2. When the polymerization was carried out using CTA 2, the characteristic pale yellow solution remained during the polymerization, and the polymer was obtained as a pale yellow powder after precipitation in methanol. The resulting poly(2MNVIn) showed a symmetrical unimodal SEC peak (see Supporting Information, Figure S6) with a relatively narrow molecular weight distribution ($M_w/M_n = 1.25$, $M_n = 3400$). The number-average molecular weight is comparable to the theoretical value ($M_{n,theory} = 4300$) calculated from the monomer/CTA molar ratio and the monomer conversion using eq 2, while achieving only 26% conversion even after 24 h. The poly(2MNVIn) obtained with CTA 1 showed broader polydispersity compared to that with CTA 2. This is most probably due to the fact that the 1-phenylethyl radical, a secondary radical, produced from CTA 2 is more easily formed than the primary benzyl radical expelled from CTA 1, resulting in the faster consumption of CTA and uniform initiation. The polymerization with CTA 3 afforded the poly(2MNVIn) with relatively low conversion and broad polydispersity (conversion = 28%, $M_w/M_n = 1.36$). It was reported that steric factors, radical stability, and polar factors all appeared to play an important role in determining the leaving group ability of R[•] (transfer coefficient) and the effectiveness of RAFT agents.^{37,58} Among three xanthate-type CTAs, the tertiary cyanoalkyl xanthate (CTA 3) should have the highest transfer

coefficient. In order to obtain a nearly monodispersed product, the leaving ability of the R group in CTA 3 must be balanced with the ability of the electron-deficient leaving radical ($R = 2$ -cyanopropyl-2-yl) to reinitiate polymerization of 2MNVIn that has an electron-donating substitute. Although the leaving ability of the secondary R group in CTA 2 is lower than that with CTA 3, CTA 2 may show good balance between the leaving ability and reinitiation ability from the electron-donating phenylethyl moiety that are stabilized by aromatic conjugation. As expected, the polymerizations with the dithiocarbamate-type and dithioester-type mediating agents (CTA 4 and CTA 5) provided the polymers with broader polydispersities. These results support our strategy that unfavorable chain transfer and termination reactions due to the high reactivity of the propagating 2MNVIn radicals could be suppressed by the MADIX/RAFT process through an increased stability of the CTA by conjugation and a destabilized intermediate radical center using xanthates. Because of the electron-donating indole pendant group, the 2MNVIn propagating radical is relatively unstable and is a poor homolytic leaving group. By using *O*-ethyl xanthate as the CTA, one can increase the electron density at the radical center and avoid the possibility of a resonance stabilization of the radical, resulting in the destabilization of the intermediate radical. This phenomenon helps to attain a counterbalance of the instability of the growing 2MNVIn radical to give fragmentation via the release of the leaving group. The conjugation of lone electron pairs on the oxygen atom with the double bond is responsible for the increased stability of the xanthate-type CTA. Same strategies were reported to be applicable for the controlled radical polymerization of the *O*-vinyl monomer, *O*-vinyl acetate.^{42–44}

In attempt to increase both monomer conversion and molecular weight, the polymerizations of 2MNVIn with CTAs were conducted for a prolonged time (48 h). In all cases, higher conversions with increased molecular weights were achieved for 48 h. In the case of the polymerization with CTA 2, poly-(2MNVIn) having a relatively narrow polydispersity and a controlled molecular weight ($M_n = 6300$, $M_w/M_n = 1.31$) was obtained with a moderate conversion (50%) after 48 h. These results indicate that the xanthate-type mediating agent (CTA 2) is efficient for the preparation of poly(2MNVIn) with relatively low polydispersity. The ability of the xanthate-type CTA 2 to control 2MNVIn polymerization may be correlated with the electron density on the central carbon atom of the xanthate and preferable fragmentation of the secondary 1-phenylethyl radical from the intermediate. Note that CTA 2 was successfully employed as a RAFT agent for well-controlled radical polymerization of a typical *N*-vinyl monomer, *N*-vinylcarbazole.⁴¹ In the next stage, therefore, we focused on the xanthate-mediated controlled radical polymerization of 2MNVIn using CTA 2 under various conditions.

Optimization of Conditions for RAFT Polymerization of 2MNVIn. In a previous publication, we demonstrated that toluene, 1,4-dioxane, and DMF were effective solvents for the controlled radical polymerization of a representative *N*-vinyl monomer, *N*-vinylcarbazole.⁴¹ Here, RAFT polymerization of 2MNVIn using CTA 2 was examined in various solvents under different monomer concentrations with the aim of increasing the polymerization rate. Generally, the way to reach higher conversion within reasonable polymerization time is to increase the monomer concentration, whereas this often leads to an increase in the viscosity, resulting in the loss of the controlled character, especially at high conversion. Solvent effects on radical polymerization originate from various factors, such as

Table 3. Effects of Solvent and Monomer Concentration on RAFT Polymerization of 2-Methyl-*N*-vinylindole (2MNVIn) with 2,2'-Azobis(isobutyronitrile) (AIBN) in the Presence of *O*-Ethyl-*S*-(1-phenylethyl)dithiocarbonate (CTA 2) for 24 h^a

run	solvent	<i>M</i> (g/mL)	conv ^b (%)	<i>M_n</i>		
				theory ^c	SEC ^d	<i>M_w</i> / <i>M_n</i> ^d
1	1,4-dioxane	0.62	66	10 600	7800	2.13
2	1,4-dioxane	0.31	26	4300	3400	1.25
3	1,4-dioxane	0.16	20	3400	2900	1.25
4	1,4-dioxane	0.08	8	1500	1000	1.27
5	DMF	0.62	70	11 200	8500	1.78
6	DMF	0.31	23	3800	2500	1.33
7	DMF	0.08	0			
8	toluene	0.62	88	14100	11000	3.35
9	toluene	0.31	45	7300	5900	1.41
10	toluene	0.08	9	1600	1700	1.24

^a [2MNVIn]₀/[CTA 2]₀/[AIBN]₀ = 200/2/1, AIBN = 2,2'-azobis(isobutyronitrile), 2MNVIn = 2-methyl-*N*-vinylindole, CTA 2 = *O*-ethyl-*S*-(1-phenylethyl)dithiocarbonate. ^b Calculated by ¹H NMR in CDCl₃. ^c The theoretical molecular weight ($M_{n,theory}$) = (MW of 2MNVIn) × [2MNVIn]₀/[CTA]₀ × conv + (MW of CTA). ^d Number-average molecular weight (M_n) and molecular weight distribution (M_w/M_n) were measured by size-exclusion chromatography (SEC) using polystyrene standards in THF.

polarity, interaction between the polymer (or monomer) and the solvent, salvation of a transition state (or intermediate) that may have polar characteristics, and complexation between the propagating radical (or monomer) and the solvent. In particular, radical–solvent complexes are expected to be favored in systems containing an unstable radical intermediate (propagating poly-(2MNVIn) radical in this system), in which complexation may lead to stabilization. The solvent may also affect the diffusion-controlled termination, and thus the termination rate coefficient may be strongly altered.

We investigated the influence of the polymerization solvent and monomer concentration in terms of the monomer conversion, molecular weights, and the polydispersity of the resulting poly(2MNVIn). Keeping the CTA 2/AIBN molar ratio of 2 and a monomer-to-CTA ratio of 100, the concentration of 2MNVIn was changed from 0.08 to 0.62 g/mL ([2MNVIn]₀ = 1.6 mol/L = 0.31 g/mL). The results are summarized in Table 3. At low concentrations (0.08–0.31 g/mL) in dry 1,4-dioxane, the polymerization proceeded homogeneous conditions, and the viscosity was low enough to ensure efficient stirring by the magnetic bar in the reaction mixture. Under the concentrations, the polymerizations were relatively slow (conversion <30% after 24 h), in comparison with these conventional radical polymerization (conversion = 69% under similar conditions, run 3 in Table 1), whereas the resulting poly(2MNVIn)s showed symmetrical SEC peaks with low polydispersities ($M_w/M_n = 1.25–1.27$). Higher monomer concentration (0.62 g/mL) resulted in faster polymerization, and 66% conversion was reached under the same conditions. However, the resulting polymer had a broader polydispersity ($M_w/M_n = 2.13$) with a shoulder SEC peak at a high molecular weight region, indicating that higher monomer concentration leads to less control of the polymerization. A similar tendency was also observed in the polymerization in toluene. At 0.31 g/mL monomer concentration, a polymer having relatively narrow polydispersity ($M_w/M_n = 1.41$) and controlled molecular weights ($M_{n,GPC} = 5900$, $M_{n,theory} = 7300$) was obtained in a moderate conversion (45%), while a higher concentration (0.62 g/mL) led to an increase in the monomer conversion and broadness of the polydispersity. Note that commercial dehydrated dioxane was stored in the dark and employed carefully in this study because of the possible effect of peroxide impurities in the solvent.⁵⁹ We also compared selected polymerizations in commercial dry dioxane and a

Table 4. Effects of Temperature and Chain Transfer Agent/Initiator Molar Ratio on RAFT Polymerization of 2-Methyl-*N*-vinylindole (2MNVIIn) Using 2,2'-Azobis(isobutyronitrile) (AIBN) and *O*-Ethyl-*S*-(1-phenylethyl)dithiocarbonate (CTA 2) in 1,4-Dioxane for 24 h^a

run	temp (°C)	[CTA 2] ₀ /[AIBN] ₀	conv ^b (%)	<i>M_n</i>		<i>M_w</i> / <i>M_n</i> ^d
				theory ^c	SEC ^d	
1	45	2	5	1000		
2	60	2	26	4300	3400	1.25
3	80	2	65	10500	8600	1.98
4	45	5	<1			
5	60	5	13	2300	2000	1.20
6	80	5	20	3400	1600	1.40

^a [2MNVIIn]₀/[CTA 2]₀ = 100/1, [AIBN]₀ = 7.8×10^{-3} and 3.1×10^{-3} mol/L, [CTA 2]₀ = 1.6×10^{-2} mol/L, [2MNVIIn]₀ = 1.6 mol/L. AIBN = 2,2'-azobis(isobutyronitrile), 2MNVIIn = 2-methyl-*N*-vinylindole, CTA 2 = *O*-ethyl-*S*-(1-phenylethyl)dithiocarbonate. ^b Calculated by ¹H NMR in CDCl₃. ^c The theoretical molecular weight (*M_{n,theory}*) = (MW of 2MNVIIn) × [2MNVIIn]₀/[CTA]₀ × conv + (MW of CTA). ^d Number-average molecular weight (*M_n*) and molecular weight distribution (*M_w*/*M_n*) were measured by size-exclusion chromatography (SEC) using polystyrene standards in THF.

purified one, suggesting the negligible effect of peroxide impurities in this system (see Supporting Information, Table S2). When the polymerization was conducted in DMF, which is a strong proton-accepting solvent and is known to act as a complex-breaking (hydrogen bond-breaking) solvent, the monomer conversion was relatively low (23%) at 0.31 g/mL for 24 h, while the conversion reached 70% at 0.62 g/mL with broad polydispersity. The pronounced concentration dependence is seen in all solvents, even if the dielectric constants of dioxane (2.2) and toluene (2.2) are significantly different from that of DMF (36.7). Taking into account the solvent-independent formation of poly(2MNVIIn)s having broader polydispersities with higher conversion at higher monomer concentration (0.62 g/mL), the effect of the solvent on the diffusion-controlled termination may be negligible in this system. These results suggest the limited effects of the polarity, hydrogen bond, and radical-solvent complexation on the RAFT polymerization of 2MNVIIn in the solvents used in this study.

The influence of the polymerization temperature was examined at different CTA-to-initiator ratios, [CTA]₀/[AIBN]₀ = 2 and 5, keeping the monomer-to-CTA ratio at a constant value of [2MNVIIn]₀/[CTA]₀ = 100/1. The results are summarized in Table 4. Note that the [CTA]₀/[AIBN]₀ ratio frequently plays a crucial role in determining the overall success of a RAFT polymerization. In general, decreasing the initiator concentration (increasing the [CTA]₀/[I]₀ ratio) leads to control of the polymerization because termination reactions will be disfavored. Because chain transfer reactions have no effect on the overall polymerization rate, the rate of polymerization should be a function of the initiator concentration as in conventional radical polymerization and independent of the CTA. The RAFT process does not induce inherent retardation phenomena because it does not rely on a persistent radical effect. Only in special cases are inhibition and rate retardation phenomena observed in RAFT polymerization. A higher CTA-to-initiator ratio occasionally provides a longer polymerization time. The rate retardation is attributed to the main equilibrium after all the initial CTA have been transformed into macro-CTA (so-called macro-RAFT agent) and may therefore be ascribed to different stabilities of the intermediate radicals in the main equilibrium. The polymerization at [CTA]₀/[AIBN]₀ = 2 at 80 °C afforded the polymer with higher monomer conversion (65%) and increased molecular weight (run 3), compared to that at 60 °C, while the resulting

Table 5. Effect of [M]/[CTA 2] Ratio on RAFT Polymerization of 2-Methyl-*N*-vinylindole (2MNVIIn) with 2,2'-Azobis(isobutyronitrile) (AIBN) and *O*-Ethyl-*S*-(1-phenylethyl)dithiocarbonate (CTA 2) in 1,4-Dioxane at 60 °C for 48 h^a

run	[M] ₀ /[CTA 2] ₀	conv ^b (%)	<i>M_n</i>		<i>M_w</i> / <i>M_n</i>	
			theory ^c	GPC ^d	GPC-RALLS ^e	GPC-RALLS ^e
1	100	50	8100	6300	8000	1.31
2	150	47	11300	7500	11000	1.24
3	200	42	13400	8900	13100	1.22
4	250	49	19500	10400	19400	1.25

^a [CTA 2]₀/[AIBN]₀ = 1/2, [M]₀ = 1.6 mol/L, 2MNVIIn = 2-methyl-*N*-vinylindole, CTA 2 = *O*-ethyl-*S*-(1-phenylethyl)dithiocarbonate. ^b Calculated by ¹H NMR in CDCl₃. ^c Theoretical molecular weight (*M_{n,theory}*) = (MW of M) × [M]₀/[CTA]₀ × conv + (MW of CTA). ^d Determined by size-exclusion chromatography (SEC) using polystyrene standards in THF. ^e Determined by GPC-RALLS measurement.

polymer had a bimodal molecular weight distribution (see Supporting Information, Figure S6). The increase in the polymerization rate at higher temperature may be due to the higher primary radical concentration at the initial stage and the increase in the propagation rate coefficient. In contrast, the increased bimolecular termination may be caused by a significant increase in radical flux at high temperature. This behavior can be also explained by the assumption that increasing the temperature leads to an increase in the radical reactivity, resulting in the decreased selectivity of the various radical reactions to promote unfavorable side reactions, particularly in the heterocyclic moiety. Another possible explanation is that higher polymerization temperature causes a remarkable increase in the fragmentation rate coefficient, leading to an increased number of active propagation radicals. This phenomenon is apparently different from the xanthate-mediated radical polymerization of *N*-vinylcarbazole, in which good control of the polymerization can be attained at higher temperature (90 °C). This is an indication that the absence of the additional phenyl group in NVIn derivatives, compared with *N*-vinylcarbazole, affects the controllability of the polymerization. In the next stage, we examined the polymerization of 2MNVIIn at a higher [CTA]₀/[AIBN]₀ ratio. Unfortunately, low monomer conversions were obtained at [CTA]₀/[AIBN]₀ = 5, regardless of the polymerization temperature. These results indicate that a careful choice of the polymerization conditions, such as polymerization solvent, monomer concentration, temperature, and [M]₀/[CTA]₀ ratio, is required to achieve controlled radical polymerization of 2MNVIIn using CTA 2.

Control of Molecular Weights. With a view to preparing poly(2MNVIIn)s over a wide range of molar mass, different degrees of polymerization were targeted. For this purpose, the polymerization of 2MNVIIn was conducted at different [2MNVIIn]₀/[CTA 2]₀ ratios between 100 and 250, while the AIBN/CTA 2 molar ratio was held constant at 1/2. When the polymerizations were conducted in 1,4-dioxane at 60 °C for 48 h, the conversions were nearly 40–50% (determined by ¹H NMR spectroscopy), as shown in Table 5. The number-average molecular weights of the poly(2MNVIIn)s increase with the [M]/[CTA] ratio, and the molecular weight distributions remain narrow (*M_w*/*M_n* = 1.21–1.33), indicating the feasibility of controlling the molecular weights. In all cases, the SEC traces are unimodal with no evidence of high molecular weight species (see Supporting Information, Figure S7).

In all cases, the experimental molecular weights are lower than the theoretical ones. These discrepancies may result from the difference in hydrodynamic volume between poly(2MNVIIn)s and the linear polystyrene standards used for GPC calibration.

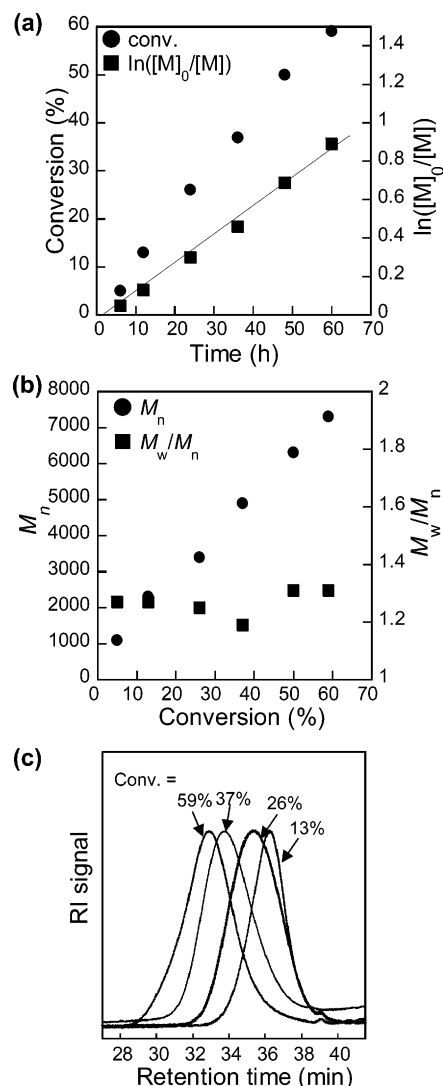


Figure 1. (a) Time–conversion (circles) and first-order kinetic (squares) plots for the polymerization of 2-methyl-*N*-vinylindole (2MNVIn) with 2,2′-azobis(isobutyronitrile) (AIBN) in the presence of *O*-ethyl-*S*-(1-phenylethyl)dithiocarbonate (CTA 2) in 1,4-dioxane at 60 °C at $[2\text{MNVIn}]_0/[CTA\ 2]_0 = 100$ and $[CTA]_0/[AIBN]_0 = 2$ ($[AIBN]_0 = 7.8 \times 10^{-3}$ mol/L, $[CTA\ 2]_0 = 1.6 \times 10^{-2}$ mol/L, and $[2\text{MNVIn}]_0 = 1.6$ mol/L). (b) Number-average molecular weight (circles) and polydispersity (squares) as a function of conversion. (c) Evolution of SEC traces with conversion.

Another possible explanation is that the number of living polymer chains is larger than that of the CTA due to an initiator-derived chain. To clarify this point, GPC with a right-angle laser light scattering detector (GPC-RALLS) was utilized for the determination of the absolute molecular weights of representative samples. As shown in Table 5, the molecular weights determined by GPC/RALLS are higher than the apparent ones obtained by conventional GPC. There were no significant differences between $M_{n,\text{GPC-RALLS}}$ and $M_{n,\text{calcd}}$, suggesting that the number of living polymer chains is comparable to that of the CTA. These results suggest good control of the polymerization of 2MNVIn, leading to the belief that the molecular weight of the indole-containing polymers can be easily adjusted by the monomer-to-CTA ratio under suitable conditions.

Polymerization Kinetics. The controlled/living character of the polymerization of 2MNVIn was studied by performing kinetics investigations in the presence of CTA 2 in dry 1,4-dioxane at 60 °C. Figure 1a shows the variations in the monomer conversion and $\ln([M]_0/[M])$ vs polymerization time for the

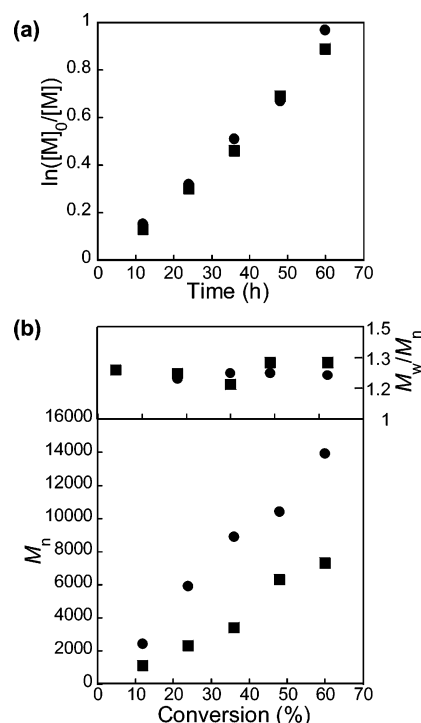


Figure 2. (a) First-order kinetic plots and (b) number-average molecular weight and polydispersity as a function of conversion at different monomer-to-chain transfer agent ratios, $[2\text{MNVIn}]_0/[CTA\ 2]_0 = 100$ (squares) and 250 (circles). $[CTA]_0/[AIBN]_0 = 2/1$, $[2\text{MNVIn}]_0 = 1.6$ mol/L, $[CTA\ 2]_0 = 1.6 \times 10^{-2}$ and 6.2×10^{-3} mol/L.

polymerizations at $[2\text{MNVIn}]_0/[CTA]_0/[AIBN]_0 = 200/2/1$. A linear first-order kinetic plot is seen up to about 60% conversion. As shown in Figure 1b, a linear increase in the number-average molecular weight with conversion reveals a constant number of propagating chains throughout the polymerization and the absence of a degenerative chain transfer reaction. The SEC traces (refractive index) of poly(2MNVIn)s obtained at different reaction times are shown in Figure 1c. A progressive increase in the molar mass with conversion with narrow unimodal SEC peaks ($M_w/M_n = 1.19\text{--}1.31$) is clearly seen, as normally evidenced for a controlled/living polymerization. Note that a shoulder peak at high molecular weight region appears at higher conversion (>70%, see Supporting Information, Figure S8), which is most probably due to combination of the growing polymer chains during a longer reaction time. Although the coupling reaction is considered to be a dominant factor in the formation of the poly(2MNVIn) with bimodal distribution and broad polydispersity, another possibility involves unfavorable side reactions on the heterocyclic ring in the resulting polymer. For example, a backbiting attack of propagating species at the 2- and 3-position of the indole ring was reported to take place during radical and cationic polymerizations to afford cyclic indole structures.²⁴ It must also be noted that the polymerization of 2MNVIn using CTA 2 is apparently slower than that of a typical *N*-vinyl monomer, *N*-vinylcarbazole, suggesting the remarkable effect of the monomer structure on both the polymerization rate and controllability.

The polymerization behavior was also compared at different targeted polymerization degrees, $[M]_0/[CTA\ 2]_0 = 250$ and 100, under the same conditions ($[CTA\ 2]_0/[AIBN]_0 = 2$). Both cases show the linear pseudo-first-order kinetic plots (Figure 2a), and there is no significant difference in the polymerization rate. The number-average molecular weights increase with the conversion, maintaining low polydispersity, as shown in Figure 2b. The molecular weights of poly(2MNVIn) obtained at $[M]_0/[CTA]_0$

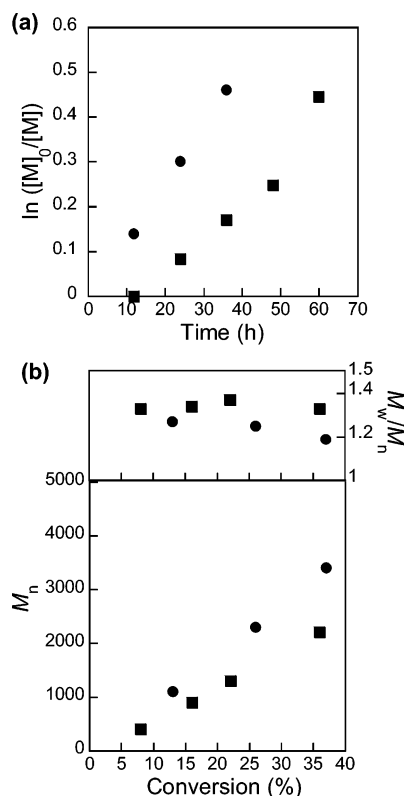


Figure 3. (a) First-order kinetic plots and (b) number-average molecular weight and polydispersity as a function of conversion at different chain transfer agent-to-initiator ratios, $[CTA\ 2]_0/[AIBN]_0 = 5$ (squares) and 2 (circles). $[2MNVI]_0/[AIBN]_0 = 200$, $[2MNVI]_0 = 1.6$ mol/L, and $[AIBN]_0 = 7.8 \times 10^{-3}$ mol/L.

$= 250$ are reasonably higher than those at $[M]_0/[CTA]_0 = 100$. These results suggest that the molecular weights can be easily controlled by the $[M]_0/[CTA]_0$ ratio and the monomer conversion, although the ratio has no significant influence on the polymerization rate and controlled character.

In both cases, induction periods are seen in the pseudo-first-order kinetic plots at 60 °C, as shown Figure 2a. The induction period roughly estimated simply by extrapolating the linear part of each curve to the time axis is about 4 h in both cases. In order to clarify the inhibition and retardation phenomena, the polymerization kinetics was investigated at different chain transfer agent-to-initiator ratios, $[CTA\ 2]_0/[AIBN]_0 = 2$ and 5, keeping the monomer-to-initiator ratio at a constant value of $[2MNVI]_0/[AIBN]_0 = 100/1$. Under these conditions, the concentrations of the monomer and initiator are constant ($[2MNVI]_0 = 1.6$ mol/L and $[AIBN]_0 = 7.8 \times 10^{-3}$ mol/L), and the CTA concentration is substantially different ($[CTA\ 2]_0 = 1.6 \times 10^{-2}$ and 4.1×10^{-2} mol/L, respectively). As shown in Figure 3a, the induction-period is about 11 h at $[CTA\ 2]_0/[AIBN]_0 = 5$, while it apparently decreases to less than 2.5 h at $[CTA]_0/[AIBN]_0 = 2$. This is an indication that both the induction period and the polymerization rate, namely inhibition and retardation, are apparently affected by the ratio.

There is an ongoing debate on the mechanism that causes the inhibition and retardation.^{46,58,60–64} The consumption of CTA and reversible fragmentation of intermediate to produce the reinitiating R^* fragment are referred to as the “preequilibrium”, which is correlated closely with the induction period (Scheme 2). The dependence of the inhibition period on the CTA/initiator ratio might be related to that of the rate of conversion of the initial RAFT agent. Other possible explanations include slow fragmentation of the initiating leaving group

radical, slow reinitiation by the expelled radical, increased stability of the intermediate radical (with and without intermediate radical termination), tendency of the expelled radical to add to the CTA rather than to the monomer, and impurities in the CTA.^{64–68} In general, chain transfer reactions have no effect on the overall polymerization rate. The rate of polymerization should be a function of initiator concentration as in conventional radical polymerization (half-order with respect to the initiator) and independent of the CTA. However, rate retardation, caused by a lower propagating radical concentration than observed in an analogous reaction without CTA, is observed in several RAFT polymerizations. The rate retardation is ascribed to different stabilities of the intermediate radicals (**4**) in the main equilibrium (Scheme 2). In this system, the $[CTA]_0/[AIBN]_0$ ratio has a remarkable effect on the polymerization rate. There are two main justifications for the rate retardation in RAFT polymerizations: side reactions, involving the intermediate radicals, and slow fragmentation of the intermediate radicals. In our system, less stabilized intermediate radicals may lead to intermediates that are slow to undergo fragmentation. The unstable growing 2MNVI radical may be related to the slow fragmentation. For a further understanding of the phenomena one can read a recent review.⁵⁸

Chain Extension. An important criterion of the controlled/living character of the polymerization is the successful extension of a chain from a preformed polymer chain as a macro-CTA. To examine this point, the dithiocarbonate-terminated poly(2MNVI) prepared independently by the polymerization using CTA 2 was employed as a macro-CTA for chain extension experiments. We used a low-molecular-weight poly(2MNVI) ($M_n = 2300$, $M_w/M_n = 1.25$), and the monomer concentration (0.31 g/1.0 mL = 1.6 mol/L) was adjusted to achieve a homogeneous reaction system without a significant increase in the solution viscosity during the polymerization. The initiator: macro-CTA molar ratio was maintained at 1:2. After the chain extension, the resulting product was analyzed by SEC and compared to the original macro-CTA. The CTA-derived initiator may produce the polymer with CTA fragments at the polymer chain ends, whereas the AIBN-derived initiator may produce the polymer with an initiator fragment at the α -chain end and the xanthate group at the ω -chain end. When the chain extension was performed at 60 °C at the ratio $[2MNVI]_0/[macro-CTA]_0/[AIBN]_0 = 400/2/1$, the monomer conversion was 26% after 24 h, and the polymer was isolated by precipitation in methanol. The extended polymer exhibited a symmetrical SEC peak with a low polydispersity ($M_w/M_n = 1.35$) (see Supporting Information, Figure S9).

The chain extension was also conducted using poly(2MNVI) macro-CTA having a higher molecular weight ($M_n = 6800$, $M_w/M_n = 1.35$) at different $[M]_0/[macro-CTA]_0$ ratios for longer polymerization time (48 h). Figure 4 shows clear shifts in the SEC traces toward higher molecular weight regions after the chain extensions. Tiny tailing can be seen in SEC traces of the products, suggesting that a small amount of residual low molecular weight dead chains remains in the final product. Nevertheless, the polydispersity remained below 1.45, regardless of the conditions. Further, the molecular weights of the resulting polymers could be simply adjusted by the composition of the $[2MNVI]_0/[macro-CTA]_0$ ratio in the feed (Table 6). These results suggest that most of the chain ends of the poly(2MNVI) are functionalized with xanthate end groups, which can be used as a macro-CTA for a further chain extension reaction.

RAFT Polymerization of *N*-Vinylindole. A monosubstituted *N*-vinylindole, 2MNVI, has been polymerized successfully via

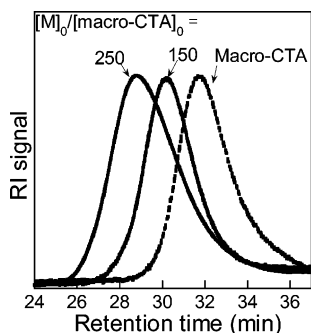


Figure 4. SEC traces of the parent poly(2MNVIn) macro-CTA (dotted trace, $M_n = 6,800$, $M_w/M_n = 1.35$, conversion = 48%) obtained at the ratio $[2MNVIn]_0/[CTA\ 2]_0/[AIBN]_0 = 400/2/1$ at 60 °C for 48 h and the chain extended polymer (solid traces, $[2MNVIn]_0/[macro-CTA\ 2]_0 = 250/1$ and $150/1$) obtained after the polymerization with 2MNVIn at the ratio $[macro-CTA]_0/[AIBN]_0 = 2/1$ for 48 h.

RAFT polymerization using CTA 2 to afford the polymers having low polydispersity and predetermined molecular weights. However, the control of the radical polymerization of NVIn was limited, as can be seen in Table 7. For example, the polymerization of NVIn using CTA 2 under the conditions used for controlled radical polymerization of 2MNVIn gave a polymer having a relatively broader polydispersity ($M_w/M_n = 1.52$). The monomer conversion was less than 42% even after the polymerization at 60 °C for 48 h. The same tendency was observed in the polymerizations of NVIn using CTA 1 and CTA 3. In both cases, the monomer conversions were low (<35%) even after 48 h, and the resulting poly(NVIn)s had relatively broad polydispersities ($M_w/M_n = 1.4$ – 2.0). For the conventional radical polymerization of NVIn without CTA, in contrast, a relatively high-molecular-weight homopolymer with a broader polydispersity index ($M_n = 12\,000$, $M_w/M_n = 3.54$) was obtained at a high conversion (conversion = 77%) after 48 h. The difference in the conversion and molecular weights of the polymers obtained in the presence and absence of CTA supports the possibility of achieving the controlled character of the polymerization. Further investigations are required to achieve controlled radical polymerization of NVIn.

Formation of Charge-Transfer Complexes. The resulting polymers were characterized in terms of their optical and thermal properties. At first we investigated the capability of the polymers, poly(NVIn) and poly(2MNVIn), to afford charge transfer (CT) complexes with typical organic acceptors, such as 7,7,8,8-tetracyanoquinodimethane (TCNQ), tetracyanoethylene (TCNE), and 2,3-dichloro-5,6-dicyano-1,4-benzoquinone (DDQ). The formation of a CT complex is a crucial point for the employment of the resulting polymers as photoconductive matrices in a photorefractive composite material.²² The UV–vis spectra were recorded in CH_2Cl_2 solutions ($[acceptor] = [indole\ unit] = 4.2 \times 10^{-3}$ mol/L) containing equimolar amounts of the two components, i.e., the organic acceptor and the indole repeating unit in the polymers. Actually, a remarkable color change was observed on the addition of TCNQ from an almost transparent polymer solution to a pale yellow, which is slightly darker than the yellow color of the original TCNQ (see Supporting Information, Figure S10). In the cases of the complexations with TCNE, the transparent TCNE solution was varied to deep blue or purple by mixing with the polymer solutions. These color changes of the solutions were detected without any microscopic precipitation, when TCNQ and TCNE were employed as acceptors. In contrast, sedimentation accompanying the color change from the pale brown DDQ solution

into dark purple (or dark green) was observed after mixing the polymer solutions with DDQ.

Figure 5 depicts the CT absorbance spectra of poly(NVIn) ($M_n = 5200$, $M_w/M_n = 1.45$) and poly(2MNVIn) ($M_n = 5900$, $M_w/M_n = 1.41$) in CH_2Cl_2 ($[acceptor] = [indole\ unit] = 4.2 \times 10^{-3}$ mol/L). The absorption maxima of the CT complexes and the molar absorption coefficients are summarized in Table 8. When TCNQ was employed as an acceptor, broad CT absorption bands are observed between 490 and 780 nm with a maximum at 680 nm, as shown in Figure 5a,d. The peak intensity is slightly higher than that of TCNQ, whereas there is no significant change in the maximum peak position (680 nm for the complex and 684 nm for TCNQ). Both TCNQ and TCNQ/polymer complexes show a strong absorption attributed to pure TCNQ at $\lambda < 490$ nm. At higher concentration (1.3×10^{-2} mol/L) (see Supporting Information, Figure S11), the asymmetric bands with the two transitions ($\lambda_{max} = 564$ and 680 nm) were seen in the CT complex using TCNQ and poly(NVIn). Note that the peak intensities of TCNQ/polymer complexes were apparently lower than those of the complexes with other acceptors, suggesting relatively weak complexations (see Supporting Information Figure S12).

In the cases of the complexations with TCNE, strong CT absorption bands were detected between 450 and 860 nm (Figure 5b,e). The longer wavelengths of the CT complexes were significantly different from the TCNE-free species. We also observed a remarkable difference in the CT absorptions between the methyl-substituted product, poly(2MNVIn), and the unsubstituted one. The CT spectrum for poly(2MNVIn) with TCNE shows a sharp absorption with a maximum at 543 nm and a broad maximum at 720 nm, whereas the complex with poly(NVIn) shows broad absorption with a maximum at 573 nm. The low-energy component is known to be related to the HOMO (highest occupied molecular orbital)–LUMO (lowest unoccupied molecular orbital) transition. In contrast, the higher energy band is attributed to a transition involving the second higher occupied molecular orbital of the donor molecules.²²

Because microscopic precipitations were observed in the cases of the complexation of DDQ with the polymer solutions, the filtrates, which were dark green solutions, were used for CT absorption measurement. As shown in Figure 5c,f, the poly(NVIn)/DDQ exhibits a CT absorption spectrum at longer wavelength (500–800 nm), which shifts from the strong DDQ band at $\lambda < 500$ nm. On the contrary, the peak of poly(2MNVIn)/DDQ complex shifts to a shorter wavelength area, which is actually located between the poly(2MNVIn) and DDQ. To obtain further information on the CT complexes of DDQ with the polymers, the dark purple precipitates formed just after mixing were isolated by filtration. After drying in vacuo at room temperature for 24 h, the isolated complexes were obtained as dark purple powders (yield = 42% for poly(NVIn)/DDQ and 66% for poly(2MNVIn)/DDQ). These complexes were insoluble in THF, $CHCl_3$, MeOH, hexane, and H_2O . Figure 6 shows the FT-IR spectra of the DDQ, the polymers, and their complexes. The C=O stretching band of DDQ ($1674\ cm^{-1}$) moves slightly to $1702\ cm^{-1}$ in the isolated complex of poly(NVIn) and DDQ, suggesting the interaction of the acceptor and the indole moiety. In contrast, the isolated poly(2MNVIn)/DDQ complex exhibits a characteristic broad peak at 2100 – $3900\ cm^{-1}$ with a negligible C=O stretching peak. Similar results were reported in electrically conductive CT complexes, in which the IR spectra were sharp for poor conductors and very broad for good conductors.⁶⁹ These results indicate that the structure and property of the

Table 6. Polymerization of 2-Methyl-*N*-vinylindole (2MNVIn) Using Macro-CTA and 2,2'-Azobis(isobutyronitrile) (AIBN) in 1,4-Dioxane at 60 °C

run	macro-CTA ^a	[M]/[macro-CTA]	time (h)	conv ^b (%)	M_n^c theory	M_n^d SEC	M_w/M_n^d
1	poly(2MNVIn) 1	200/1	24	26	10 500	8 900	1.35
2	poly(2MNVIn) 2	150/1	48	55	19 800	15 400	1.18
3	poly(2MNVIn) 2	200/1	48	44	20 600	17 000	1.44
4	poly(2MNVIn) 2	250/1	48	46	24 900	19 600	1.45

^a Poly(2MNVIn) 1: $M_n = 2300$, $M_w/M_n = 1.25$, conversion = 13%; poly(2MNVIn) 2: $M_n = 6800$, $M_w/M_n = 1.35$, conversion = 48%. ^b Calculated by ¹H NMR in CDCl₃. ^c Calculated by the conversion and the molecular weight of the poly(2MNVIn) macro-CTA. ^d Number-average molecular weight (M_n) and molecular weight distribution (M_w/M_n) were measured by size-exclusion chromatography (SEC) using polystyrene standards in THF.

Table 7. Polymerization of *N*-Vinylindole (NVIn) Using Different Chain Transfer Agents (CTAs) with 2,2'-Azobis(isobutyronitrile) (AIBN) in 1,4-Dioxane at 60 °C^a

run	CTA ^b	time (h)	conv ^c (%)	M_n^d theory	M_n^e SEC	M_w/M_n^e
1		48	77		12000	3.54
2	CTA 1	24	25	3800	6600	1.71
3	CTA 1	48	34	5100	7300	1.98
4	CTA 2	24	20	3100	3100	1.52
5	CTA 2	48	42	6200	5200	1.45
6	CTA 3	24	14	2200	4800	1.55
7	CTA 3	48	33	4900	6000	1.45

^a [NVIn]₀/[CTA]₀/[AIBN]₀ = 200/2/1, [AIBN]₀ = 7.8×10^{-3} mol/L, [CTA]₀ = 1.6×10^{-2} mol/L, [NVIn]₀ = 1.6 mol/L. ^b CTA 1 = *S*-benzyl-*O*-ethylthiocarbonate, CTA 2 = *O*-ethyl-*S*-(1-phenylethyl)dithiocarbonate, and CTA 3 = *O*-ethyl-*S*-(2-cyano)prop-2-yl)dithiocarbonate. ^c Calculated by ¹H NMR in CDCl₃. ^d Theoretical molecular weight ($M_{n,theory}$) = (MW of M) \times [M]₀/[CTA]₀ \times conv + (MW of CTA). ^e Number-average molecular weight (M_n) and molecular weight distribution (M_w/M_n) were measured by size-exclusion chromatography (SEC) using polystyrene standards in THF.

complexes are affected by the polymer structure and that the ability to create a complex with the indole unit is in the order of DDQ > TCNE > TCNQ.

The polymer having low polydispersity prepared by RAFT polymerization was compared to the conventional polymer, which was prepared independently by a conventional radical polymerization with AIBN. No significant difference was detected in the absorption spectra of the CT complexes at 200–800 nm (see Supporting Information, Figure S13). This means that the thermal properties can be manipulated simply by the molecular weights of poly(2MNVIn)s, as mentioned in the next section, without changing the optical property and the ability for the CT complex formation. Note that the poly(NVIn) and poly(2MNVIn) exhibited a pale blue fluorescence upon excitation at 365 nm, which were different from the corresponding monomers (see Supporting Information, Figure S14).

Thermal Properties. The thermal properties of the resulting polymers were determined by differential scanning calorimetry (DSC) and thermogravimetric analysis (TGA) measurements. The glass transition temperature (T_g) of poly(2MNVIn)s having different molecular weights were analyzed by DSC, and the results are shown in Figure 7a. A reasonable dependence of T_g on the molecular weights was observed. The T_g value of poly(2MNVIn) having relatively high molecular weights ($M_n = 14\,300$ and $M_w/M_n = 1.65$) was found to be 185 °C, which was apparently higher than that having low molecular weights ($T_g = 158$ °C, $M_n = 5100$ and $M_w/M_n = 1.27$). The same tendency was observed in the poly(2MNVIn)s obtained by free radical polymerization. The T_g value ($T_g = 210$ °C, $M_n = 30\,200$ and $M_w/M_n = 2.05$) obtained in this study is apparently higher than the reported value ($T_g = 184$ °C,²² $M_n = 4500$, $M_w/M_n = 1.6$), which may be due to the effect of the molecular weight. The effect of the molecular weight on T_g can be quantified using the following equation: $T_g = T_g(\infty) - K/M_n$. According to the equation, the theoretical values of representative poly(2MNVIn)s

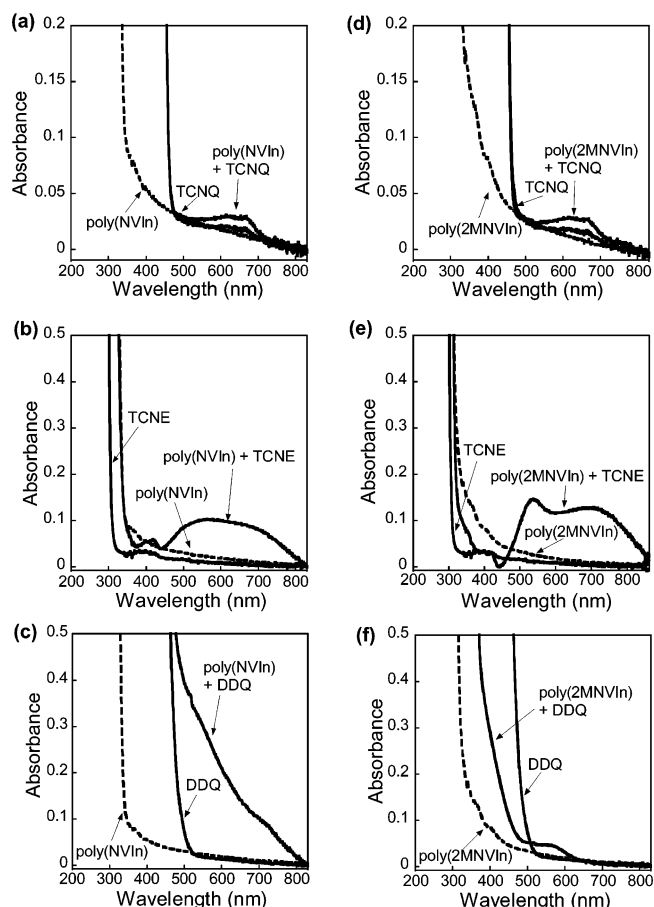


Figure 5. Absorption spectra of acceptors, polymers, and their CT complexes (1/1 molar ratio) in CH₂Cl₂ ([acceptor] = [indole unit] = 4.2×10^{-3} mol/L): (a–c) poly(*N*-vinylindole) [poly(NVIn)], (d–f) poly(2-methyl-*N*-vinylindole) [poly(2MNVIn)], (a, d) 7,7,8,8-tetracyanoquinodimethane (TCNQ), (b, e) tetracyanoethylene (TCNE), (c, f) 2,3-dichloro-5,6-dicyano-1,4-benzoquinone (DDQ).

Table 8. Molar Absorption Coefficient and λ_{max} of Poly(NVIn) and Poly(2MNVIn) with Acceptor^a

run	polymer	acceptor	λ_{max}^b (nm)	ϵ^c (mol L ⁻¹ cm ⁻¹)
1	poly(NVIn)	TCNQ	680	3.61
2	poly(2MNVIn)	TCNQ	680	3.61
3	poly(NVIn)	TCNE	573	12.3
4	poly(2MNVIn)	TCNE	543	17.5

^a CT complexes of polymers with acceptors in CH₂Cl₂ ([acceptor] = [indole unit] = 4.2×10^{-3} mol/L). ^b Measured by UV–vis spectroscopy. ^c Molar absorption (ϵ) = A/cd (A = absorbance of λ_{max} , c = concentration (mol/L), d = length of cell width (cm)).

prepared by RAFT polymerization can be calculated to be 158 °C ($M_n = 5100$), 174 °C ($M_n = 8900$), and 182 °C ($M_n = 14\,300$), which are in good agreement with the observed values (158, 171, and 185 °C, respectively). The calculated value of $T_g(\infty)$ is 195 °C for the poly(2MNVIn). The lower T_g values of poly(2MNVIn) compared to a typical photoconductive polymer,

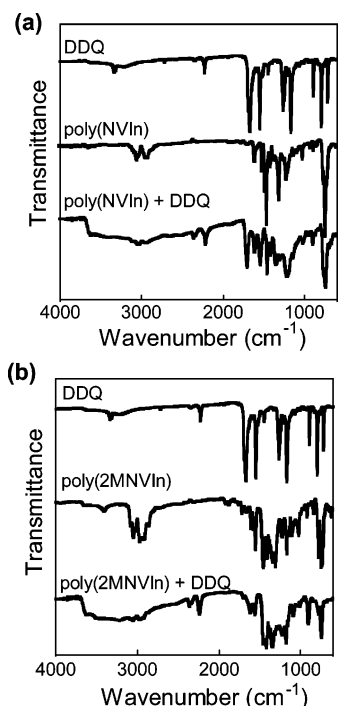


Figure 6. FT-IR spectra of (a) DDQ, poly(NVIn), and their isolated CT complex and (b) DDQ, poly(2MNVIn), and their CT complex.

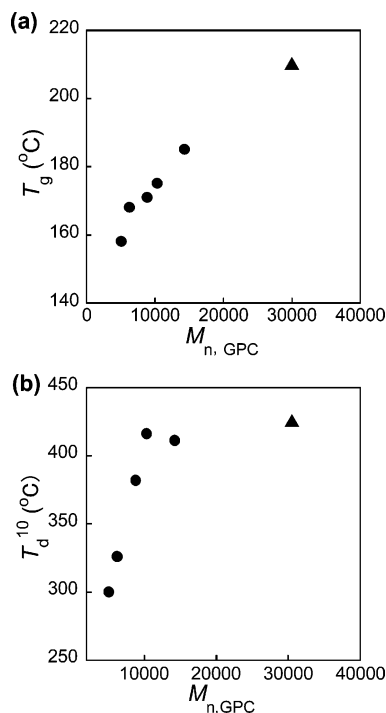


Figure 7. Dependence of number-average molecular weights (M_n) on (a) glass transition temperature (T_g) and (b) the temperature for 10% weight loss. Poly(2MNVIn)s obtained by free radical polymerization (triangle, $M_n = 30\,200$, $T_g = 210\text{ }^\circ\text{C}$, $T_d^{10} = 430\text{ }^\circ\text{C}$) and RAFT polymerizations (circles, other M_n s).

poly(*N*-vinylcarbazole) ($T_g = 227\text{ }^\circ\text{C}^{22}$), are crucial when these polymers are used as photorefractive materials at room temperature. Hence, the feasibility to control the T_g value by the molecular weights makes them potentially promising candidates for poly(*N*-vinylcarbazole) replacement in photorefractive materials.

Thermal stability of the resulting polymers was analyzed under nitrogen. The poly(2MNVIn) was stable up to $300\text{ }^\circ\text{C}$,

and then the thermal degradation of the main chain started; the results are shown in Supporting Information (Figure S15). The temperature for 10% weight loss of high molecular weight poly-(2MNVIn) ($M_n = 13\,900$ and $M_w/M_n = 1.25$) under a nitrogen atmosphere is $415\text{ }^\circ\text{C}$, which is almost the same as that of the polymer obtained by conventional radical polymerization ($T_d^{10} = 428\text{ }^\circ\text{C}$, $M_n = 30\,200$ and $M_w/M_n = 2.05$). Poly(NVIn) prepared by RAFT polymerization showed a similar thermal stability ($T_d^{10} = 394\text{ }^\circ\text{C}$, $M_n = 14\,300$ and $M_w/M_n = 1.65$). The temperature (T_d^{10}) decreased with the decreasing molecular weights (Figure 7b) and finally reached the lowest value for low molecular weight poly(2MNVIn) ($T_d^{10} = 300\text{ }^\circ\text{C}$, $M_n = 5900$ and $M_w/M_n = 1.27$) (see Supporting Information, Figure S15). This is an indication that the chemical structure of the end group has a significant influence on the degradation behavior of the low molecular weight product, while the effect is negligible on the polymers having higher molecular weights ($M_n > 10\,000$).

Conclusion

We investigated the radical polymerization of three *N*-vinylindole derivatives, NVIn, 2MNVIn, and 3MNVIn, using various CTAs. The poly(2MNVIn)s with controlled molecular weights and low polydispersities were obtained by polymerization with a careful choice of reaction conditions in the presence of CTA 2 as a xanthate-type CTA. Good control of the polymerization was confirmed by the linear first-order kinetic plot, the molecular weight controlled by the monomer/CTA molar ratio, linear increase in the molecular weight with the conversion, and the ability to extend the chain by a second addition of the monomer. The UV-vis spectra of the polymers showed additional absorptions due to the formation of CT complexes with acceptors. It was found that the structure and properties of the complexes with poly(2MNVIn) are different from those with poly(NVIn) and that the ability to form the complexes is in the order of DDQ > TCNE > TCNQ. In particular, strong CT absorption bands were obtained at longer wavelength (450–860 nm) without any microscopic precipitation, when TCNE was used as an acceptor. The glass transition temperature (T_g) of poly(2MNVIn) was arbitrarily adjusted in the range of $150\text{--}220\text{ }^\circ\text{C}$ by changing the molecular weights. These polymers having well-defined structures can provide various functional materials with unique electronic and optical properties for various applications, such as photorefractive materials.

Acknowledgment. The authors acknowledge Professor Seigou Kawaguchi for help with excess refractive index increment (dn/dc) measurement.

Supporting Information Available: Figures showing ^1H and ^{13}C NMR spectra of the monomers and polymers, SEC traces of poly(2MNVIn)s obtained at different temperatures (60 and $80\text{ }^\circ\text{C}$), $[\text{M}]_0/[\text{CTA } 2]_0$ ratios, polymerization times, chain extension, appearance of samples illuminated under visible and UV light, absorption spectra of the CT complexes at higher concentration and the complexes with different polymers, TGA thermograms of poly(2MNVIn)s, tables summarizing the date for all kinetic investigations, comparison of ^1H NMR and ^{13}C NMR signals of *N*-vinyl monomers, and polymerization results in commercial dry dioxane and purified one. This material is available free of charge via the Internet at <http://pubs.acs.org>.

References and Notes

- (1) Humphrey, G. R.; Kuethe, J. T. *Chem. Rev.* **2006**, *106*, 2875–2911.
- (2) Borschberg, H. R. *Curr. Org. Chem.* **2005**, *9*, 1465–1491.
- (3) Camilleri, M. *Aliment. Pharmacol. Ther.* **2001**, *15*, 277–289.
- (4) Kawasaki, T.; Higuchi, K. *Nat. Prod. Rep.* **2005**, *22*, 761–793.
- (5) Horton, D. A.; Bourne, G. T.; Smythe, M. L. *Chem. Rev.* **2003**, *103*, 893–930.
- (6) Huffman, J. W.; Padgett, L. W. *Curr. Med. Chem.* **2005**, *12*, 1395–1411.
- (7) Beaulieu, P. L.; Bos, M.; Bousquet, Y.; DeRoy, P.; Fazal, G.; Gauthier, J.; Gillard, J.; Goulet, S.; McKercher, G.; Poupart, M. A.; Valois, S.; Kukolj, G. *Bioorg. Med. Chem. Lett.* **2004**, *14*, 967–971.
- (8) Nefzi, A.; Ostresh, J. M.; Houghten, R. A. *Chem. Rev.* **1997**, *97*, 449–472.
- (9) Weedon, A. *Advances in Photochemistry*; Wiley/VCH: New York, 1997; Vol. 22.
- (10) Milanese, M.; Viterbo, D.; Albini, A.; Fasani, E.; Bianchi, R.; Barzaghi, M. *J. Org. Chem.* **2000**, *65*, 3416–3425.
- (11) Perez-Prieto, J.; Bosca, F.; Galian, R. E.; Lahoz, A.; Domingo, L. R.; Miranda, M. A. *J. Org. Chem.* **2003**, *68*, 5104–5113.
- (12) Gonzalez-Bejar, M.; Stiriba, S. E.; Domingo, L. R.; Perez-Prieto, J.; Miranda, M. A. *J. Org. Chem.* **2006**, *71*, 6932–6941.
- (13) Ahmed, I. T. *Spectrochim. Acta, Part A* **2006**, *63*, 416.
- (14) Takani, M.; Takeda, T.; Yajima, T.; Yamauchi, O. *Inorg. Chem.* **2006**, *45*, 5938–5946.
- (15) Bowyer, P. K.; Black, D. S.; Craig, D. C.; Rae, A. D.; Willis, A. C. *J. Chem. Soc., Dalton Trans.* **2001**, 1948–1958.
- (16) Lo, K. K. W.; Lee, T. K. M.; Zhang, K. Y. *Inorg. Chim. Acta* **2006**, *359*, 1845–1854.
- (17) Lo, K. K. W.; Tsang, K. H. K.; Hui, W. K.; Zhu, N. Y. *Chem. Commun.* **2003**, 2704–2705.
- (18) John, A.; Palaniappan, S. *Polymer* **2005**, *46*, 12037–12039.
- (19) Pandey, P. C.; Prakash, R. J. *Electrochem. Soc.* **1998**, *145*, 999–1003.
- (20) Xu, J. K.; Hou, J.; Zhang, S. S.; Zhang, R.; Nie, G. M.; Pu, S. Z. *Eur. Polym. J.* **2006**, *42*, 1384–1395.
- (21) Ohoka, M.; Ohkita, H.; Ito, S.; Yamamoto, M. *Polym. Bull. (Berlin)* **2004**, *51*, 373–380.
- (22) Brustolin, F.; Castelvetro, V.; Ciardelli, F.; Ruggeri, G.; Colligiani, A. *J. Polym. Sci., Part A: Polym. Chem.* **2001**, *39*, 253–262.
- (23) Nomori, H.; Hatano, M.; Kambara, S. *Polym. Lett.* **1966**, *4*, 623–628.
- (24) Priola, A.; Gatti, G.; Cesca, S. *Makromol. Chem.* **1979**, *180*, 1–11.
- (25) Hwang, J.; Sohn, J.; Lee, J. K.; Lee, J. H.; Chang, J. S.; Lee, G. J.; Park, S. Y. *Macromolecules* **2001**, *34*, 4656–4658.
- (26) Moon, H.; Hwang, J.; Kim, N.; Park, S. Y. *Macromolecules* **2000**, *33*, 5116–5123.
- (27) Hwang, J.; Moon, H.; Seo, J.; Park, S. Y.; Aoyama, T.; Wada, T.; Sasabe, H. *Polymer* **2001**, *42*, 3023–3031.
- (28) Hashidzume, A.; Harada, A. *Polymer* **2005**, *46*, 1609–1616.
- (29) Hashidzume, A.; Harada, A. *Polymer* **2006**, *47*, 3448–3454.
- (30) Sata, T.; Nomura, R.; Masuda, T. *Polym. Bull. (Berlin)* **1998**, *41*, 395–399.
- (31) Gipstein, E.; Hewett, W. A. *Macromolecules* **1969**, *2*, 82–85.
- (32) Priola, A.; Gatti, G.; Santi, G.; Cesca, S. *Makromol. Chem.* **1979**, *180*, 13–24.
- (33) Matyjaszewski, K.; Xia, J. H. *Chem. Rev.* **2001**, *101*, 2921–2990.
- (34) Kamigaito, M.; Ando, T.; Sawamoto, M. *Chem. Rev.* **2001**, *101*, 3689–3745.
- (35) Hawker, C. J.; Bosman, A. W.; Harth, E. *Chem. Rev.* **2001**, *101*, 3661–3688.
- (36) Chiefari, J.; Chong, Y. K.; Ercole, F.; Krstina, J.; Jeffery, J.; Le, T. P. T.; Mayadunne, R. T. A.; Meijs, G. F.; Moad, C. L.; Moad, G.; Rizzardo, E.; Thang, S. H. *Macromolecules* **1998**, *31*, 5559–5562.
- (37) Moad, G.; Rizzardo, E.; Thang, S. H. *Aust. J. Chem.* **2005**, *58*, 379–410.
- (38) McCormack, C. L.; Lowe, A. B. *Acc. Chem. Res.* **2004**, *37*, 312–325.
- (39) Perrier, S.; Takolpuckdee, P. J. *J. Polym. Sci., Part A: Polym. Chem.* **2005**, *43*, 5347–5393.
- (40) Favier, A.; Charreyre, M. T. *Macromol. Rapid Commun.* **2006**, *27*, 653–692.
- (41) Mori, H.; Ookuma, H.; Nakano, S.; Endo, T. *Macromol. Chem. Phys.* **2006**, *207*, 1005–1017.
- (42) Coote, M. L.; Radom, L. *Macromolecules* **2004**, *37*, 590–596.
- (43) Stenzel, M. H.; Cummins, L.; Roberts, G. E.; Davis, T. R.; Vana, P.; Barner-Kowollik, C. *Macromol. Chem. Phys.* **2003**, *204*, 1160–1168.
- (44) Nguyen, T. L. U.; Eagles, K.; Davis, T. P.; Barner-Kowollik, C.; Stenzel, M. H. *J. Polym. Sci., Part A: Polym. Chem.* **2006**, *44*, 4372–4383.
- (45) Wan, D. C.; Satoh, K.; Kamigaito, M.; Okamoto, Y. *Macromolecules* **2005**, *38*, 10397–10405.
- (46) Moad, G.; Chiefari, J.; Chong, Y. K.; Krstina, J.; Mayadunne, R. T. A.; Postma, A.; Rizzardo, E.; Thang, S. H. *Polym. Int.* **2000**, *49*, 993–1001.
- (47) Ladaviere, C.; Dorr, N.; Claverie, J. P. *Macromolecules* **2001**, *34*, 5370–5372.
- (48) Gaillard, N.; Guyot, A.; Claverie, J. J. *J. Polym. Sci., Part A: Polym. Chem.* **2003**, *41*, 684–698.
- (49) Destarac, M.; Taton, D.; Zard, S. Z.; Saleh, T.; Six, Y. *Adv. Controlled/Living Radical Polym.* **2003**, *854*, 536–550.
- (50) Shi, L. J.; Chapman, T. M.; Beckman, E. J. *Macromolecules* **2003**, *36*, 2563–2567.
- (51) Bouhadir, G.; Legrand, N.; Quiclet-Sire, B.; Zard, S. Z. *Tetrahedron Lett.* **1999**, *40*, 277–280.
- (52) Mori, H.; Nakano, S.; Endo, T. *Macromolecules* **2005**, *38*, 8192–8201.
- (53) Chiefari, J.; Mayadunne, R. T. A.; Moad, C. L.; Moad, G.; Rizzardo, E.; Postma, A.; Skidmore, M. A.; Thang, S. H. *Macromolecules* **2003**, *36*, 2273–2283.
- (54) Mori, H.; Iwaya, H.; Nagai, A.; Endo, T. *Chem. Commun.* **2005**, *38*, 4872–4874.
- (55) Chong, Y. K.; Krstina, J.; Le, T. P. T.; Moad, G.; Postma, A.; Rizzardo, E.; Thang, S. H. *Macromolecules* **2003**, *36*, 2256–2272.
- (56) Bogdal, D.; Jaskot, K. *Synth. Commun.* **2000**, *30*, 3341–3352.
- (57) Abele, E.; Dzenitis, O.; Rubina, K.; Lukevics, E. *Chem. Heterocycl. Compd.* **2002**, *38*, 682–685.
- (58) Barner-Kowollik, C.; Buback, M.; Charleux, B.; Coote, M. L.; Drache, M.; Fukuda, T.; Goto, A.; Klumperman, B.; Lowe, A. B.; McLeary, J. B.; Moad, G.; Monteiro, M. J.; Sanderson, R. D.; Tonge, M. P.; Vana, P. *J. Polym. Sci., Part A: Polym. Chem.* **2006**, *44*, 5809–5831.
- (59) Vana, P.; Albertin, L.; Barner, L.; Davis, T. P.; Barner-Kowollik, C. *J. Polym. Sci., Part A: Polym. Chem.* **2002**, *40*, 4032–4037.
- (60) Monteiro, M. J.; de Brouwer, H. *Macromolecules* **2001**, *34*, 349–352.
- (61) Kwak, Y.; Goto, A.; Tsujii, Y.; Murata, Y.; Komatsu, K.; Fukuda, T. *Macromolecules* **2002**, *35*, 3026–3029.
- (62) Luo, Y. W.; Wang, R.; Yang, L.; Yu, B.; Li, B. G.; Zhu, S. P. *Macromolecules* **2006**, *39*, 1328–1337.
- (63) Barner-Kowollik, C.; Quinn, J. F.; Morsley, D. R.; Davis, T. P. *J. Polym. Sci., Part A: Polym. Chem.* **2001**, *39*, 1353–1365.
- (64) Vana, P.; Davis, T. P.; Barner-Kowollik, C. *Macromol. Theory Simul.* **2002**, *11*, 823–835.
- (65) Perrier, S.; Barner-Kowollik, C.; Quinn, J. F.; Vana, P.; Davis, T. P. *Macromolecules* **2002**, *35*, 8300–8306.
- (66) Plummer, R.; Goh, Y. K.; Whittaker, A. K.; Monteiro, M. J. *Macromolecules* **2005**, *38*, 5352–5355.
- (67) Coote, M. L. *Macromolecules* **2004**, *37*, 5023–5031.
- (68) McLeary, J. B.; Calitz, F. M.; McKenzie, J. M.; Tonge, M. P.; Sanderson, R. D.; Klumperman, B. *Macromolecules* **2005**, *38*, 3151–3161.
- (69) Wheland, B. C.; Gillson, J. L. *J. Am. Chem. Soc.* **1976**, *98*, 3916–3925.

MA062839Q